minerals

MDPI

Article

Characterisation of the Hydration Products of a Chemically and Mechanically Activated High Coal Fly Ash Hybrid Cement

Grizelda du Toit [1], Elizabet M. van der Merwe [2], Richard A. Kruger [3], James M. McDonald [1] and Elsabé P. Kearsley [4,*]

[1] Centre of Product Excellence, AfriSam South Africa (Pty) Ltd., Johannesburg 1724, South Africa; grizelda.dutoit@za.afrisam.com (G.d.T.); mike.mcdonald@za.afrisam.com (J.M.M.)
[2] Department of Chemistry, University of Pretoria, Pretoria 0002, South Africa; liezel.vandermerwe@up.ac.za
[3] Richonne Consulting, P.O. Box 742, Somerset Mall 7137, South Africa; richonne@mweb.co.za
[4] Department of Civil Engineering, University of Pretoria, Pretoria 0002, South Africa
* Correspondence: elsabe.kearsley@up.ac.za; Tel.: +27-12-420-2176

Abstract: Cement companies are significant contributors of the planet's anthropogenic CO_2 emissions. With increased awareness of the substantial volume of CO_2 emissions from cement production, a variety of mitigation strategies are being considered and pursued globally. Hybrid cements are deemed to be technologically viable materials for contemporary construction. They require less clinker than that for ordinary Portland cement, leading to a decrease in CO_2 emissions per tonne of hybrid cement manufactured. The hybrids produced in this study consist of 70% siliceous coal fly ash and 30% Portland cement, and combines chemical (sodium sulphate) and mechanical (milling) activation. The aim of this work was to develop a better understanding of the hydration products formed and the resulting effect of activation on these hydration products, of hybrid coal fly ash cement pastes over an extended curing period of up to one year. The results indicated that chemical activation increases the formation of stable, well crystallised ettringite. Chemical activation as well as mechanical activation increased the rate of the pozzolanic reaction between portlandite contained in cement and coal fly ash. The application of combined chemical and mechanical activation definitely resulted in the fastest rate of portlandite consumption, hence an increased rate of the pozzolanic reaction.

Keywords: hybrid cement; coal fly ash; ettringite; pozzolanic reactivity; compressive strength

Citation: du Toit, G.; van der Merwe, E.M.; Kruger, R.A.; McDonald, J.M.; Kearsley, E.P. Characterisation of the Hydration Products of a Chemically and Mechanically Activated High Coal Fly Ash Hybrid Cement. *Minerals* **2022**, *12*, 157. https://doi.org/10.3390/min12020157

Academic Editors: Rolf Sjöblom and Chongchong Qi

Received: 15 October 2021
Accepted: 20 December 2021
Published: 27 January 2022

1. Introduction

Cement companies are significant contributors of the planet's anthropogenic CO_2 emissions. With increased awareness of the substantial volume of CO_2 emissions from cement production, a variety of mitigation strategies are being considered and pursued globally [1]. Immediate replacement of Portland cement by any of the possible alkaline cements (or any other binder) is currently not possible due to technical concerns around paste, mortar and concrete rheology or the supply of universally available, standardised quality prime cementitious raw materials. However, partial replacement i.e., hybrid cements, are deemed to be technologically viable materials for contemporary construction [2].

A hybrid coal fly ash cement is a binder with a composition between that of pozzolanic coal fly ash cement and alkali activated coal fly ash cement [3–5]. The production of hybrid cement requires less clinker than that for ordinary Portland cement, leading to a decrease in CO_2 emissions per tonne of hybrid cement manufactured. Hybrid alkaline cements is often preferred over their alkali activated counterparts because its hydration occurs at ambient temperature, and its production do not require the addition of highly alkaline chemicals, but rather rely on a safe source of alkali formed in situ (sodium hydroxide) to facilitate both the dissolution of any amorphous phases present in the source materials [5–8].

During the production of commercially available blended cement, the maximum coal fly ash content is typically constrained to 35%. This limitation is due to undesirable

performance properties such as insufficient early strength and slow strength development, which are generally ascribed to the rate of the pozzolanic reaction (pozzolanic activity) between cement and coal fly ash. This drawback results in less than half of the coal fly ash produced globally being used in cement [9–12]. Hybrid cements typically contain at least 70% fly ash by mass [13,14], and if commercially viable coal fly ash based hybrid cements are to be developed, it would be necessary to enhance the reactivity of coal fly ash. Most commercially available blended cements incorporate coal fly ash in its original form

Coal fly ash reactivity can be improved by either chemical or mechanical activation or a combination of these two techniques [5,6,15–20].

When chemical activation of coal fly ash hybrid cements are considered, factors like the type of alkaline activator used, the degree of the pozzolanic reaction, curing temperature, the presence of soluble silica, and the quantity of Fe_2O_3 (to name a few), all have an impact on the reaction kinetics, the formation and stability of secondary reaction products, and the proportion and structure of the main reaction products or gels present (or not) in the hydrated cement [19,20]. Depending on the latter, the main hydration products for coal fly ash hybrid cements may include hydrated calcium silicates (C-S-H phase) of low degree of crystallinity and variable chemical composition, hydrated aluminate phases, and in the presence of SO_4^{2-}, sulfoaluminates such as ettringite and monosulfoaluminate [21].

Mechanical activation does not have such a significant impact on the type of hydration products produced in hybrid cements, but rather improves its physical characteristics e.g., bulk and surface reactivity. It offers the possibility of changing the reactivity of solids without altering their overall chemical composition. It was shown that the reactivity of coal fly ash varies with variation in the median particle size and that it increases rapidly when the size is reduced to 5–7 μm [19,20].

Different authors have found variances in the results obtained for characterisation of the secondary products formed when making use of sodium sulphate (Na_2SO_4) as chemical activator on high coal fly ash-containing hybrid cements. The early age hydration process of a high fly ash hybrid cement which was activated with Na_2SO_4 was hypothesized by Donatello et al. [5]. In addition to the typical main hydration products, the presence of portlandite (as a result of cement hydration) and in situ formed NaOH and gypsum was reported. These authors could not confirm the presence of the hypothesized gypsum. It was also concluded that ettringite formation and its stability became inhibited as alkalinity increased at early ages (the maximum hydration period studied was 3 days) [5,6]. The verdict on the undetected gypsum was also supported and published by Garcia-Lodeiro et al. [16] and Fernández-Jiménez et al. [18] in studies completed on high fly ash-containing hybrid cements with the same activator (Na_2SO_4).

Garcia-Lodeiro et al. [14] published a comprehensive review on the hydration models for hybrid alkaline cement containing a very large proportion of alkaline cement in collaboration with Donatello and other known researchers in the field. In this publication, the reaction chemistry model for the use of an inorganic salt (Na_2SO_4) as activator for fly ash hybrid cement remained in agreement with Donatello's 2013 publication [5]. It was also noted that monocarboaluminate formed and was prevalent in the 7-day materials, and that no ettringite was detected.

Velandia et al. [22] also investigated the hydration products produced from high fly ash-containing hybrid cements (50% fly ash), adding Na_2SO_4 as a chemical activator. The results of these authors contradict that of the formerly mentioned authors in that they found that mixes activated with Na_2SO_4 had an elevated ettringite content. A noteworthy conclusion from the work done by Velandia et al. is that the Na_2SO_4 activation did not have the same effect on ettringite formation when fly ashes with higher Fe_2O_3 (~9–11%) was used compared to fly ashes with lower Fe_2O_3 content (~4–5%). The latter proved to enhance both ettringite formation and portlandite consumption.

In a more recent study by Wilinska et al. [11], the influence of chemical activators ($Ca(OH)_2$ and Na_2SO_4 used together) on hydration/activation of fly ash-cement mixtures containing about 80% of fly ash was studied. The research included early hydration periods

(3 and 24 h) and subsequent days (till 90th day of hydration). It was concluded that chemical activation promoted the precipitation of ettringite, which was visible in the XRD results of specimens hydrated for 28 days. However, the XRD peaks associated to the presence of ettringite had very low intensities at an early hydration period of 24 h, and no mention was made on the stability of the formed ettringite at later (90 days) hydration periods. Once again, chemical activation proved to enhance the development of pozzolanic activity, ettringite formation and increased the rate of precipitation of hydration products [23].

It is distinctly clear from the literature presented that, although similar hydration products are achieved to a certain extent when high fly ash containing hybrid cements are chemically activated by means of Na_2SO_4, consensus on the rapidity and stability of ettringite formation and whether its presence is still evident at very late hydration ages (beyond 28 days), has not been reached. This variance in results may very well be ascribed to the fact that the origin of the coal fly ash used affects the physical and chemical processes involved in hydration of coal fly ash hybrid cement, as much as the type of activator and activation method [21]. It is for this reason that it is important to gain a better understanding of the hydration products resulting from utilising well characterised raw materials which comply with international standards.

This work aims to investigate the effect of chemical activation (Na_2SO_4), mechanical activation (milled), as well as a combination of these activation methods on the pozzolanic activity and ettringite formation of a coal fly ash hybrid cement at specifically early, as well as later curing ages (1 day, 7-, 28-, 90-, 180 days and 1 year). The hybrids produced consist of 70% siliceous coal fly ash and 30% Portland cement. In turn this may aid to develop a better understanding of the improved mortar compressive strength characteristics of a hybrid coal fly ash cement hydrated for up to a year, which was investigated and published in previous work [24].

2. Materials and Methods

2.1. Materials

In this study a commercially available, unclassified coal fly ash, produced as a by-product during coal-fired power generation, and sourced from a South African ash beneficiation company located at a power station in the Free State province, was utilized along with Portland cement. The coal ash is EN 450 (Fly ash for concrete), category N compliant. Unclassified coal fly ash (UFA, d_{50} about 60 μm) was milled in a laboratory ball mill to produce the mechanically activated coal fly ash sample (MUFA, d_{50} about 5 μm). The Portland cement, produced by milling clinker along with approximately 10% limestone and 5% gypsum in a vertical roller mill, until a mean particle size of approximately 13 μm is achieved, was also sourced from a South African supplier, and complies with EN 197 (Composition, specifications and conformity criteria for common cements). Sodium sulphate (Na_2SO_4, anhydrous, 99%, Merck, South Africa), was used for chemical activation.

2.2. Methods

2.2.1. Hybrid Coal Fly Ash Cement Paste

Neat hybrid coal fly ash cement paste specimens for the purpose of characterisation of hydration products by means of analytical techniques were prepared by mixing 70% of dry UFA or MUFA respectively with 30% cement (MC) by mass and a constant water:binder ratio of 0.5. The pastes were chemically activated by adding 5% sodium sulphate respectively as a dry powder directly to each mix, calculated as a mass percentage of the total cementitious content [24,25]. The pastes were cast in expanded polystyrene (EPS) moulds. Each EPS mould consisted of 6 cavities (55 mm × 52 mm × 45 mm), and duplicate specimens were cast for each curing age.

The specimens were prepared for the following curing ages: 1, 7, 28, 90, 180 and 365 days. After casting, the pastes were cured in temperature controlled water tanks at 23 ± 1 °C. Upon demoulding of the specimens at the specified curing ages, they were immediately crushed into small fractured pieces and immersed into sealed isopropanol

containers for 7 days [26–28], where after they were dried at 40 °C to drive off any remaining isopropanol and stored in desiccators under vacuum in order to arrest hydration until the appropriate analyses could be performed. Hydration products of the arrested hybrid coal fly ash cement pastes were characterised using X-ray powder diffraction (XRD), Derivative Thermogravimetric analysis (DTG), Fourier transform infrared spectroscopy (FTIR) and Field Emission Scanning Electron Microscopy (FESEM).

2.2.2. Characterisation Techniques

The chemical composition of these materials was determined by X-ray Fluorescence (XRF) fused bead analysis (PANalytical Axios). The glass disk was prepared by mixing 1 g of the sample with 5 g of fluxing agent (Analytical grade $Li_2B_4O_7$) and fusing the mixture at 1000 °C. The fine powdered samples required no additional milling prior to the analysis. The loss-on-ignition (LOI) was determined by roasting the sample at 1050 °C for 1 h until a constant weight was achieved.

The particle size distribution (PSD) was obtained by laser diffraction using a Malvern Mastersizer 2000 fitted with a Scirocco 2000 sample handling unit. Scattered light data was recorded for 25 s. A refractive index of 1.68 and absorption of 1 was chosen. Size data collection was performed within the recommended 10–20% obscuration range.

X-ray powder diffraction (XRD) measurements were carried out by using a PANalytical X'Pert Pro Powder Diffractometer an X'Celerator detector and variable divergence- and fixed receiving slits, with Fe filtered Co-Kα radiation (λ = 1.789Å). The phases were identified using X'Pert Highscore plus software. The relative phase amounts (weight %) were estimated using the Rietveld method (Autoquan Program). Twenty percent silicon (Aldrich 99% pure) was also added to each sample for the determination of amorphous content. The samples were then micronized in a McCrone micronizing mill, and prepared for XRD analysis using a back loading preparation method. XRD analysis of the coal fly ash specimens cured in calcium hydroxide did not include the addition of silicon, since only the crystalline phases were identified for the purpose of the study.

Fourier transform infrared spectroscopy (FTIR) measurements were recorded with a Bruker Tensor Fourier transform infrared spectrometer by placing the finely ground samples in a diamond ATR (attenuated total reflection) cell. Data was collected from 400 cm^{-1} to 4000 cm^{-1} and data analysis was performed using OPUS 7.2 software. Thirty-two scans were signal-averaged in each interferogram.

Thermogravimetric analysis (TGA) and Derivative Thermogravimetric analysis (DTG) for this study was performed on a TGA/DSC 1 STARe system from METTLER TOLEDO. Data evaluation was performed on version 9.10 of the STARe Excellence software. Samples were heated in uncovered 70 µL alumina oxide crucibles from 40 °C to 800 °C at a dynamic heating rate of 10 °C/min. Nitrogen gas, purged at a flow rate of 20 mL/min, was used as the measurement atmosphere.

The morphology of the hybrid coal fly ash cement pastes was studied as a supplementary technique to the above-mentioned techniques, in a Zeiss Ultra SS (Germany) field emission scanning electron microscope (FESEM), operated at an acceleration voltage of 1 kV under high-vacuum conditions. Specimens cured in calcium hydroxide were dried and then procured by dipping carbon stubs into the powders. Excess powder was removed by gentle blowing with compressed nitrogen. The samples were sputter-coated with carbon (Emitech K550X Ashford, England) and placed in the microscope for examination.

2.2.3. Hybrid Coal Fly Ash Cement Mortar

Hybrid coal fly ash mortar blends for the compressive strength test work consisted of a mixture containing 75 wt. % standard reference sand (with a relative density of 2.63 g/m^3) and 25 wt. % hybrid cement (70 wt. % of the relevant coal fly ash product and 30 wt. % Portland cement. The blends were chemically activated by adding 5% sodium sulphate as a dry powder directly to each mix, calculated as a mass percentage of the total cementitious content. A constant water-to-binder (the binder only includes cement and coal fly ash) ratio

of 0.5 was maintained for all blends. Preparation, mixing and compressive strength testing of all blends were done as per EN 196-1: Methods of testing cement Part 1: Determination of strength [29]. At predetermined curing ages (1 day, 2-, 7-, 28-, 90-, 180 days and 1 year); samples were removed from the curing tanks and their compressive strength determined. Compressive strengths reported are the arithmetic mean of 6 measurements (n = 6) [24].

3. Results and Discussion

3.1. Characterization of the Starting Materials

The particle size distribution (volume % and cumulative undersize volume) of the unclassified coal fly ash (UFA), mechanically activated coal fly ash (MUFA) and cement sample, used as starting materials, is presented in Figure 1 and summarized in Table 1. It is evident that UFA is significantly coarser than MUFA and that the particle size of UFA was reduced approximately ten times upon milling to produce MUFA (Table 1). Due to the greater abundance of smaller particles, MUFA will have the larger surface area and is therefore expected to be more reactive and achieve higher compressive strength than UFA when used in cementitious binders. The Portland cement used in this study has a mean particle size of approximately 13 µm with a significantly smaller coarse fraction compared to UFA.

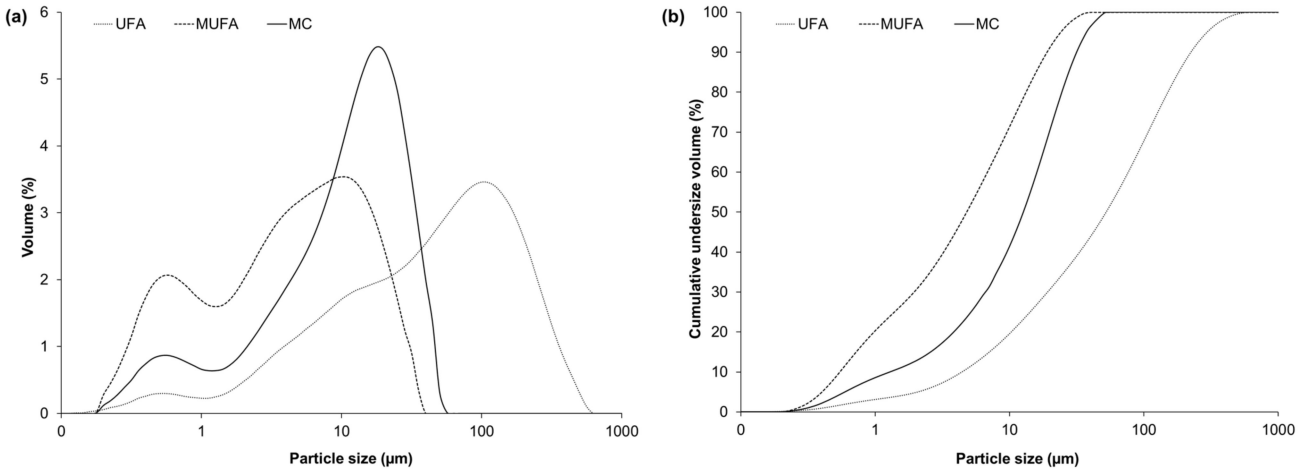

Figure 1. Particle size distribution of the coal fly ash (UFA and MUFA) and cement (MC) samples: (**a**) volume %; (**b**) cumulative undersize volume.

Table 1. Comparison of volume weighted percentile diameters of the coal fly ash (UFA and MUFA) and cement (MC) samples used as starting material.

	Diameter		
	d_{10}	d_{50}	d_{90}
UFA	4.4	52.5	224.2
MUFA	0.5	4.8	19.0
MC	1.3	12.7	31.6

The chemical (XRF) and mineralogical (XRD) compositions are presented in Table 2. While there are no major differences in chemical composition the mineralogy of UFA and MUFA differ. The coal fly ash samples consist predominantly of an amorphous alumina silicate glass phase, which is slightly higher in MUFA (61.5%) than in UFA (55.3%). The total amount of crystalline phases (mostly mullite and quartz) occur in slightly higher quantity in UFA (44.7%) than in MUFA (38.6%). The effect of milling UFA to produce MUFA decreased the mullite and quartz content slightly, accompanied by a concomitant increase of approximately 6% in the amorphous content, a result previously observed in

literature [30,31]. The composition of the Portland cement is typical of that produced in South Africa.

Table 2. Chemical composition (XRF, wt %) and mineralogical composition (XRD, wt % normalised) of the starting materials.

	UFA	MUFA	Cement		UFA	MUFA	Cement
SiO_2	54.83	54.87	20.36	Anhydrite	-	-	1.3
Al_2O_3	30.86	31.11	4.73	Belite	-	-	7.7
CaO	4.84	5.06	65.08	Alite	-	-	43.2
Fe_2O_3	3.62	3.83	2.80	Brownmillerite	-	-	12.9
MgO	1.17	1.19	1.78	Tricalcium aluminate	-	-	3.4
K_2O	0.63	0.63	0.46	Calcite	-	-	9.9
Na_2O	0.16	0.17	0.07	Gypsum	-	-	1.3
TiO	1.57	1.55	0.45	Hematite	1.0	0.8	-
Mn_2O_3	0.03	0.03	0.10	Mullite	31.5	27.5	-
P_2O_5	0.63	0.63	0.07	Quartz	12.2	10.3	0.8
SO_3	0.40	0.31	2.73	Amorphous	55.3	61.5	19.3
LOI	1.19	1.64	5.67				

The morphology of UFA and MUFA (Figure 2) indicates that spherical particles which are known to improve particle packing density in mortar and concrete [32], are more predominant in UFA (Figure 2a,b) than MUFA (Figure 2c,d), which is expected due to the milling that the MUFA sample underwent. Both specimens contained irregularly shaped particles, which may be associated to the presence of mullite and quartz (Table 2). The mechanically activated sample, MUFA has an abundance of broken spheres as well as spherical particles seemingly unaffected by the milling process. The remnants of the broken spheres may reduce the physical advantages associated with spherical morphology i.e., improved particle packing and lower water demand [9,19].

3.2. Mortar Compressive Strength of Hybrid Coal Fly Ash Cement

The mortar compressive strengths of the hybrid coal fly ash cement specimens under investigation was discussed at length in an earlier publication [24]. A summary of the compressive strength results is presented in Figure 3. During the production of hybrid cements, the coal fly ash content is limited due to low initial strength and slow strength development, ascribed to a delay in pozzolanic activity [33]. The data in Figure 3 confirms the low early strength and slow rate of strength development for the UFA hybrid, while the rate of strength development for the mechanically activated MUFA hybrid is significantly better than that of UFA. The addition of 5% sodium sulphate to produce the UFA5 (Chemically activated Unclassified Coal Fly Ash) and MUFA5 (Chemically and mechanically activated Unclassified Coal Fly Ash) hybrids was a suitable activation method for increasing early age strength (after 1 day) for both coal fly ash samples tested.

The MUFA5 hybrid achieved the highest compressive strength results at up to 28 days of curing. The MUFA5 hybrid produced compressive strengths that comply with a 32.5R (rapid early strength gain) product according to EN 197, which requires a minimum strength of 10 MPa at 2 days and 32.5 MPa at 28 days [34]. None of the other hybrids (UFA, UFA5 and MUFA) produced any strengths complying with the EN cement specification. This confirms that the combination of the characteristics that chemical and mechanical contribute to the hydrated hybrid coal fly ash cement, contributes the most to improved early age strength and rate of strength development results. It should however be noted that for the MUFA hybrid, the strength reached by the reference specimen (mechanically activated, 0% sodium sulfate) at 90 days and beyond exceeds that reached by the specimens where mechanical and chemical activation are combined. This was also true in the case of UFA at 180 and 365 days of curing. Hence, if high long term strength (beyond 90 days) is required, mechanical activation of unclassified coal fly ash, without the addition of chemical activation could be considered. The latter could be ascribed to the rapidly increased rate

at which portlandite is consumed at early curing ages upon activation, especially when combined activation is applied, making it unavailable for further pozzolanic reaction at later curing ages (see Figures 4 and 5).

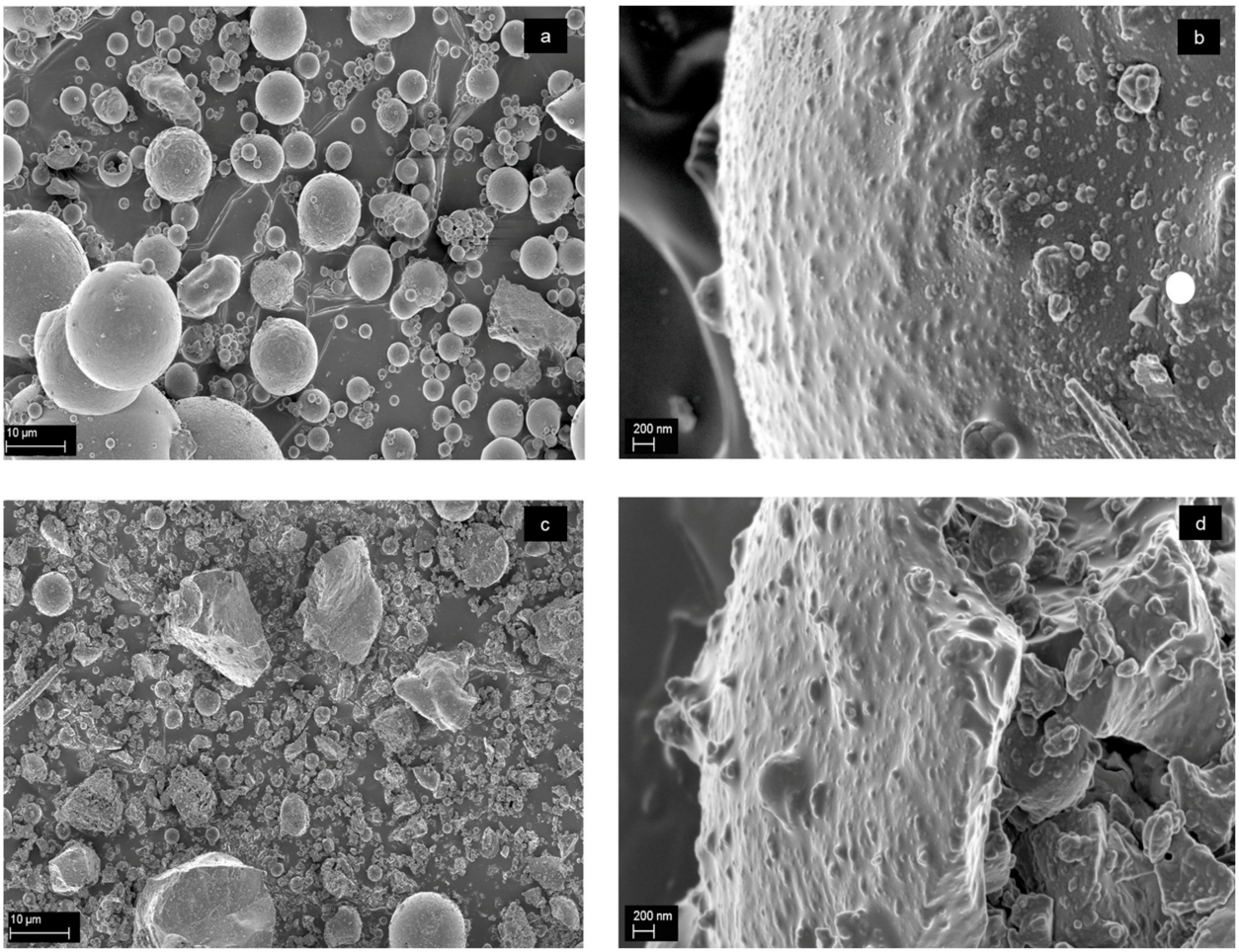

Figure 2. Scanning electron micrographs representing the morphology of untreated (**a**,**b**) UFA, and (**c**,**d**) MUFA at 3000× and 50,000× magnification respectively.

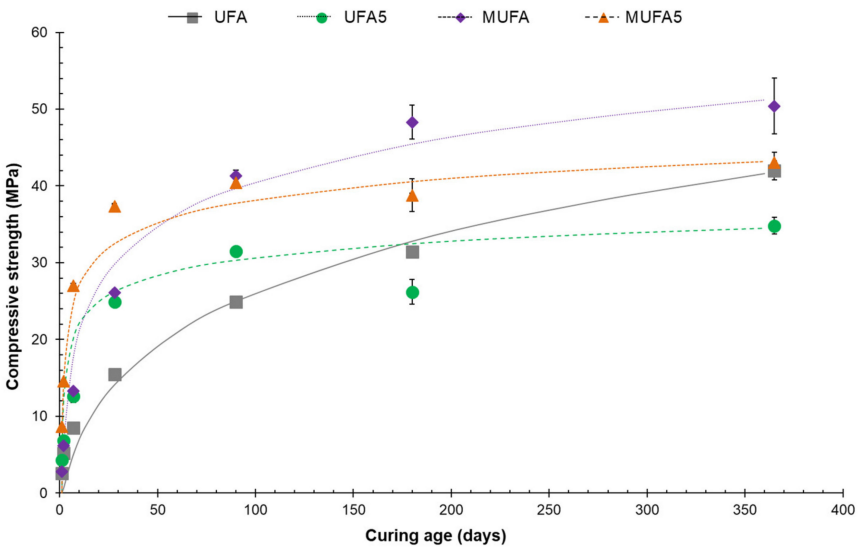

Figure 3. Mortar compressive strength (MPa) of hybrid coal fly ash cement (n = 6).

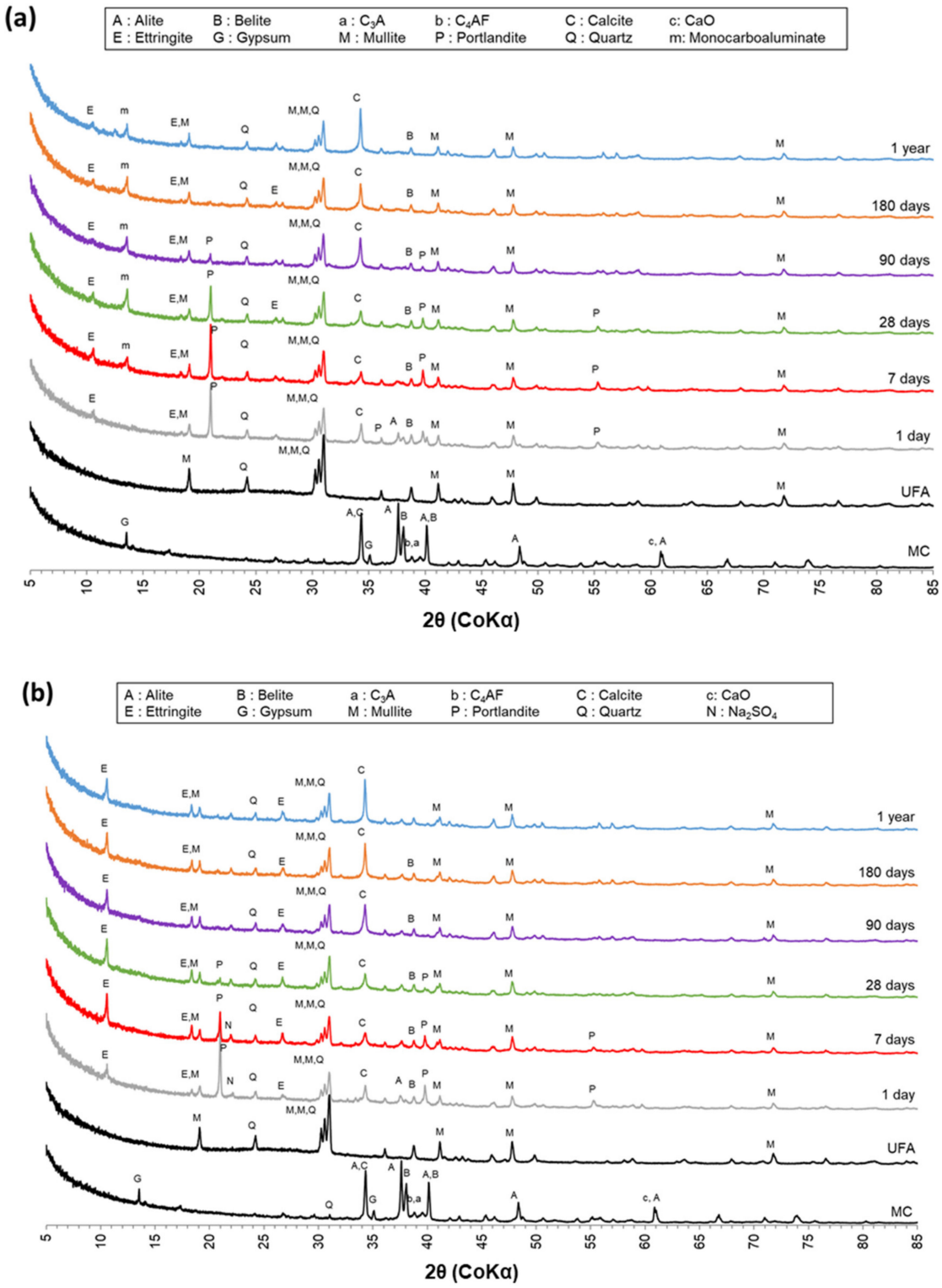

Figure 4. XRD diffractograms of anhydrous cement, UFA and hydrated (**a**) UFA and (**b**) UFA5 hybrid cement, at all curing ages tested.

3.3. Characterisation of Hydrating Hybrid Coal Fly Ash Cement Paste

The data that resulted from the application of analytical techniques used to identify the hydration products obtained for the coal fly ash hybrid cement pastes prepared, with and without chemical and mechanical activation is presented and discussed. The different characterisation techniques used (XRD, DTG, FTIR and FESEM) have different capabilities,

each supplying unique information about the hydration products. The composition of the crystalline phases in the hydration products can be determined by XRD, but the technique cannot be used to characterise amorphous phases. For this reason, DTG and FTIR analysis were used as complementary techniques, as the results obtained using these techniques are not dependent on the degree of crystallinity of the product. Where applicable, FESEM was used to observe important changes in morphologies upon hydration of the starting materials. These results were interpreted in support of the findings from the other analytical techniques.

3.3.1. X-ray Powder Diffraction (XRD) Analysis

The mineralogical composition of the cementitious materials used as starting materials were discussed in the Section 2. The diffractograms of the raw cementitious materials and the relevant hydrated specimens are presented in Figures 4 and 5. In Figure 4, the combined diffraction patterns obtained for the UFA and UFA5 hybrid cement at all of the considered hydration ages are presented. Figure 5 combines the diffraction patterns obtained for the MUFA and MUFA5 hybrid cement at all of the considered hydration ages.

The diffractograms for the anhydrous cement (MC, Figures 4 and 5) show that the material is comprised of several common crystalline cement clinker phases of which alite (C_3S) is the main component. The cement component also contains crystalline phases such as belite (C_2S), tricalcium aluminate (C_3A), brownmillerite (C_4AF), calcite ($CaCO_3$) and a small amount of gypsum ($CaSO_4 \cdot 2H_2O$). The same anhydrous cement specimen is presented for all four hybrid cement scenarios (Figures 4 and 5).

The anhydrous coal fly ash specimens (UFA and MUFA, Figures 4 and 5) exhibit the characteristic hump between the 20° and 40° 2Θ angles, attributed to the amorphous glass phase of coal fly ash [35,36], as well as diffraction lines attributed to quartz and mullite.

After 1 day of hydration, the UFA hybrid (Figure 4a) produced diffraction patterns consisting primarily of a combination of the characteristic lines identified for the raw materials, along with new hydration peaks associated with portlandite ($Ca(OH)_2$) and ettringite ($(3CaO) \cdot (Al_2O_3) \cdot 3CaSO_4 \cdot 32H_2O$)), and from 7 days onwards monocarboaluminate ($4CaO \cdot Al_2O_3 \cdot CO_3 \cdot 11H_2O$) is also present. The latter three phases are typical secondary reaction products in ordinary Portland cement hydration as well as in high coal fly ash containing cements. The peaks associated with ettringite were identified at all of the presented curing ages. A sharp peak (2Θ = 21.0°) identified as portlandite appears after 1 day of hydration, and stays prominent up to 28 days of hydration. At 90 days of curing, this peak's intensity reduces significantly and it is no longer evident at 180 days. After 28 days of hydration, most of the anhydrous cement phases have presumably been converted to a C-S-H-type gel as per normal cement hydration. This phase is unfortunately amorphous to X-rays but its existence is evident by the less intense peaks associated with anhydrous cement i.e., C_3S, C_2S, C_3A and C_4AF [37–39].

Once Na_2SO_4 have been added to the UFA hybrid (Figure 4b), it is clearly evident that the intensity of the diffraction peaks of ettringite relative to the intensity of the main diffraction peak of quartz (which is regarded as mostly unreactive) increased throughout all curing ages. Also, the previously intense portlandite peaks evident up to 28 days of curing, and to some extent 90 days in the control UFA hybrid, now appears significantly less intense at 28 days of curing and is non-existent at 90 days. The presence of monocarboaluminate (2Θ = 13.6°) is also no longer evident at any of the curing ages.

In comparison to the chemically unactivated UFA hybrid (Figure 4a), the MUFA hybrid (Figure 5a) also produces peaks identified as ettringite, portlandite and monocarboaluminate. Portlandite is identified after 1 day of hydration, although it is not as intense as for the UFA hybrid cement and is consumed before 28 days of hydration.

The MUFA5 hybrid (Figure 5b) generally displayed similar diffraction patterns to the UFA5 hybrid after chemical activation. Portlandite was consumed at an even quicker rate compared to the UFA5 hybrid, and is completely consumed after only 7 days of hydration.

The consistent presence of ettringite at all curing ages, prove that chemical activation by means of Na_2SO_4 addition increases the degree of ettringite formation which may lead to denser hybrid specimens with increased strength, as was presented in Figure 3 [24]. It is also evident that the extent of the pozzolanic reaction is increased via both chemical and mechanical activation, but more so by a combination of activation methods [22,40,41].

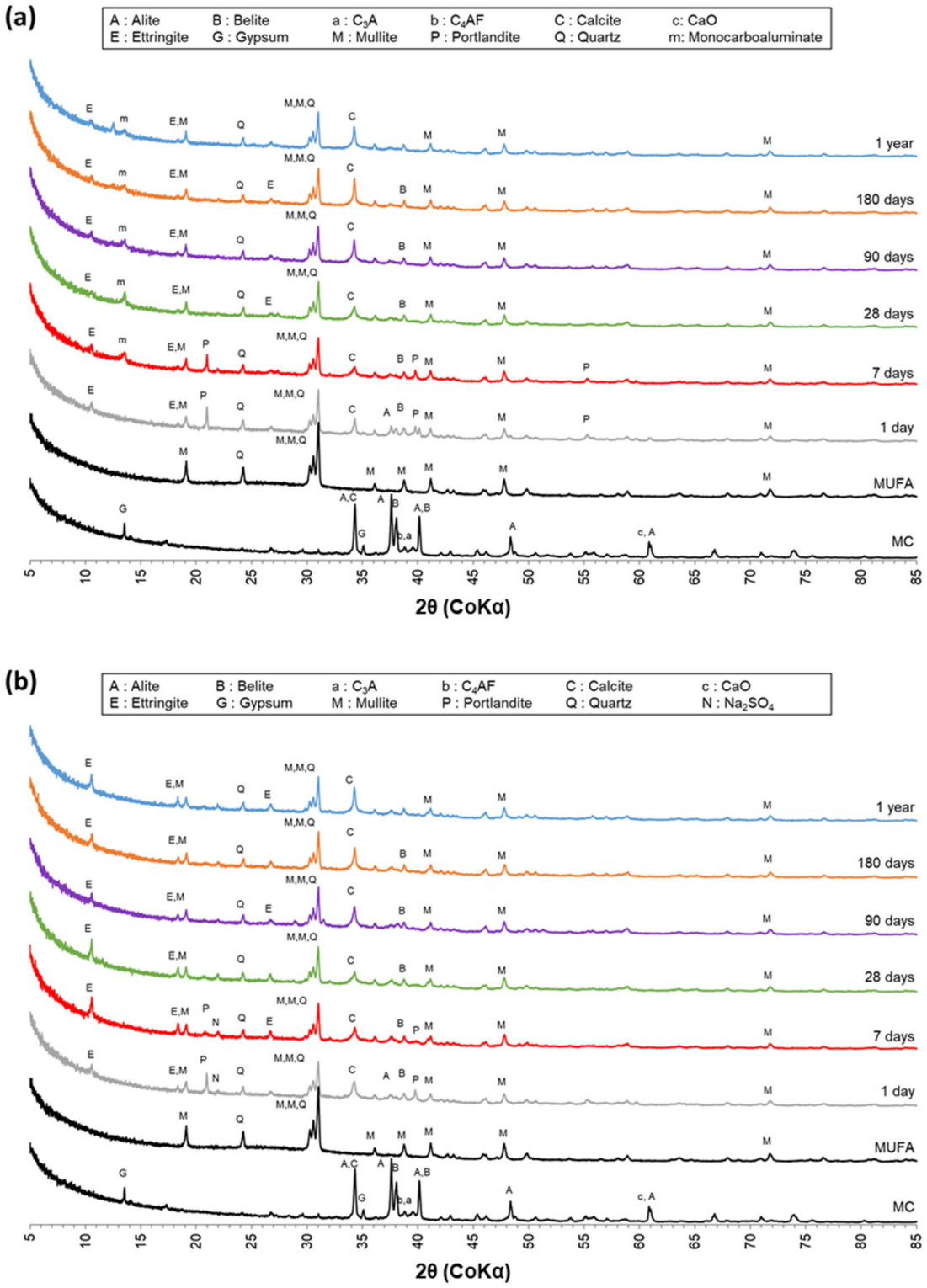

Figure 5. XRD diffractograms of anhydrous cement, MUFA and hydrated (**a**) MUFA and (**b**) MUFA5 hybrid cement, at all curing ages tested.

3.3.2. Derivative Thermogravimetric Analysis (DTG)

The rate of mass change upon heating of the coal fly ash hybrid cement pastes was studied via Derivative Thermogravimetric analysis (DTG), which is obtained mathematically from the first derivative of the thermogravimetric curve (TGA). The most prominent dehydration, dehydroxylation and decarbonation temperature regions for cement and hydrated cement is presented in Table 3 [28,42–44].

Table 3. The most prominent dehydration, dehydroxylation and decarbonation temperature regions for cement and hydrated cement [28,42–44].

	Cement Phase	Chemical Formula	Temperature Range (°C)
Dehydration <300 °C	C-S-H (Calsium silicate hydrates)	-	50–600
	Gypsum	$CaSO_4 \cdot 2H_2O$	100–120
	Ettringite	$3CaO \cdot Al_2O_3 \cdot 3CaSO_4 \cdot 32H_2O$	90–140
	Hemihydrate	$CaSO_4 \cdot 0.5H_2O$	120–130
	Monocarboaluminate	$4CaO \cdot Al_2O_3 \cdot CO_3 \cdot 11H_2O$	125–175
Dehydroxylation 400–500 °C	Portlandite	$Ca(OH)_2$	400–500
Decarbonation >600 °C	Calcium Carbonate	$CaCO_3$	600–800

The DTG curves of the four different hybrid cement pastes (UFA, UFA5, MUFA and MUFA5) at different curing ages, are presented in Figures 6 and 7. The DTG curves of the raw cementitious materials (UFA, MUFA and MC) are also shown in each graph for comparative purposes.

The DTG curve of anhydrous cement (MC; Figures 6 and 7) shows dehydration of gypsum around 120 °C, dehydroxylation of portlandite at around 444 °C and decomposition of calcite between 640–750 °C [28]. The main hydration products of the hybrid cement specimens produced in this study were identified to be C-S-H, ettringite and monocarboaluminate. Loss of chemically bound water during heating of hydrated cement samples can be observed in DTG measurements from temperatures as low as 50 °C. The dehydration of calcium silicate hydrate (C-S-H) phases is observed over a wide temperature range which may span from 50–600 °C [45,46]. Ettringite dehydrates rapidly over a much narrower temperature range around 90–120 °C [28,42,44,45]. Monocarboaluminate dehydrates between 125–175 °C [42,43]. Confirmation of the presence of ettringite by DTG is difficult due to overlapping temperature ranges for the dehydration of C-S-H and ettringite [42,43]. This may be overcome by application of a complimentary technique (e.g., XRD) to confirm the presence of ettringite prior to DTG analysis.

From the DTG curve of the UFA hybrid cement paste (Figure 6a) it can be seen that after 1 day of hydration, mass loss associated with the dehydration of C-S-H and ettringite is evident between 40–240 °C with a peak maximum at around 90 °C. This peak maximum shifted to higher temperatures with increasing curing age, which is interpreted to be due to ettringite becoming denser and more stable [44,47]. A secondary peak, due to the loss of water from monocarboaluminate, appears from 7 days of hydration at around 160 °C. The peak associated with the dehydration of portlandite at approximately 450 °C is still visible at 90 days of hydration, and to a small extent after 180 days.

When chemical activation (Na_2SO_4) is applied to the UFA hybrid (Figure 6b), the strong ettringite peak becomes more prominent compared to the UFA hybrid containing no chemical activation (Figure 6a). Dehydration of the sample hydrated up to 1 year produces a DTG curve with two peak maxima at around 90 and 110 °C. This is interpreted as a separation in the temperatures of maximum rate of dehydration of C-S-H and ettringite, since both phases are expected to occur insignificant quantities after prolonged hydration. What is also noteworthy is that the mass loss peak associated with the dehydration of

monocarboaluminate at around 160 °C is significantly smaller and less prominent. Portlandite is consumed much quicker, with the mass loss associated with the dehydration of portlandite only evident up to 28 days.

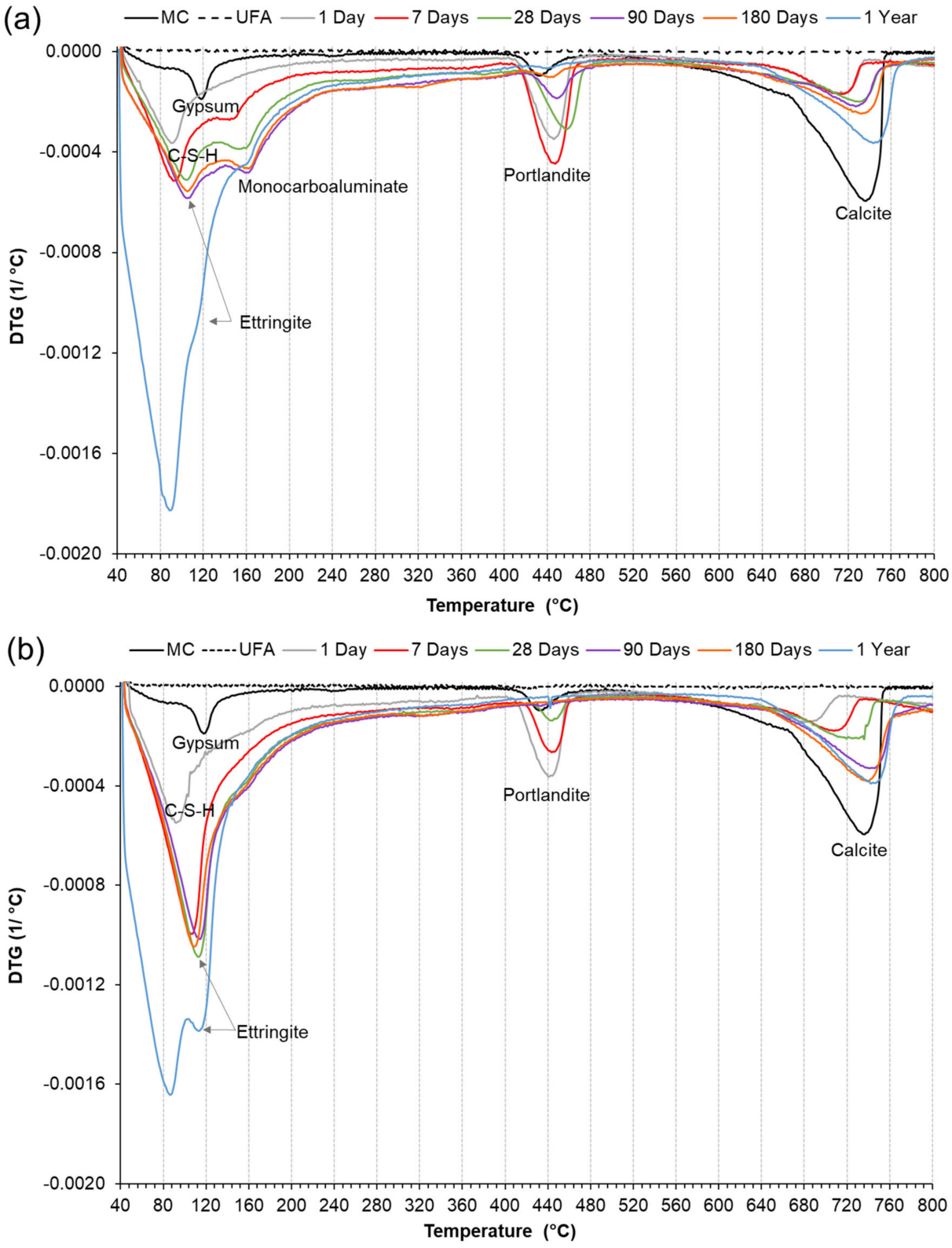

Figure 6. DTG curves of anhydrous cement (MC), UFA and hydrated (**a**) UFA and (**b**) UFA5 hybrid cement, at all curing ages tested.

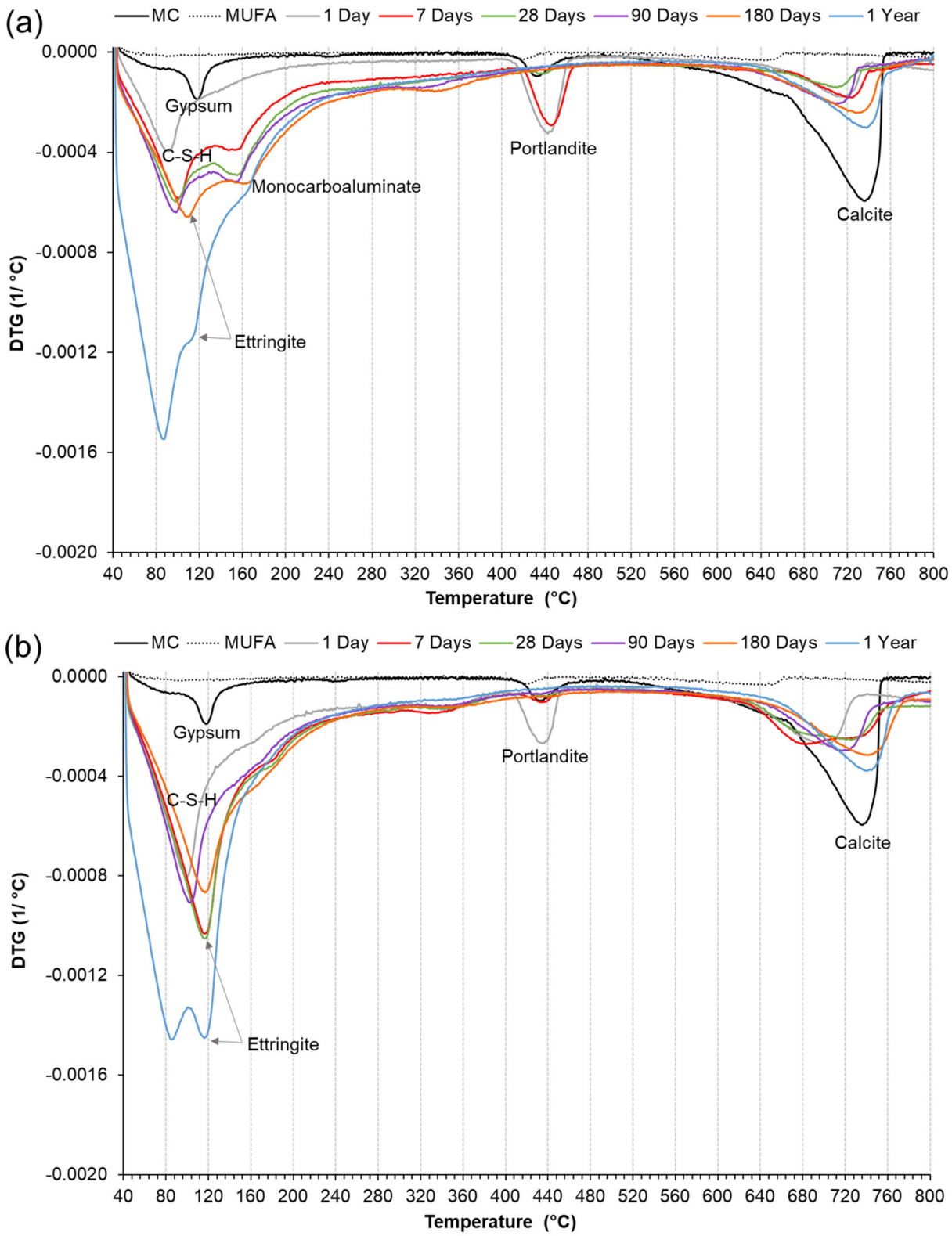

Figure 7. DTG of anhydrous cement (MC), MUFA and hydrated (**a**) MUFA and (**b**) MUFA5 hybrid cement, at all curing ages tested.

Once mechanical activation is applied to produce the MUFA hybrid, the DTG curve (Figure 7a) show that portlandite has already been consumed after 7 days. This agrees with the XRD data presented (Figure 5a). DTG curves associated with the dehydration

of C-S-H and ettringite (40–240 °C), is similar to that of the UFA and UFA5 hybrids, with separation of the peak again evident for the samples hydrated for 1 year. DTG analysis of the MUFA hybrid paste also presents a clear mass loss associated with the dehydration of calcium monocarboaluminate (approximately 160 °C), which disappears once Na_2SO_4 is added to the hybrid cement paste (MUFA5) and activation methods are combined (chemical and mechanical), as shown in Figure 7b. The mass loss associated with the dehydration of portlandite when activation methods are combined, is visible for a shorter period for the MUFA5 hybrid (1 day, Figure 7b) than for the UFA5 hybrid (28 days, Figure 6b). The addition of Na_2SO_4 as chemical activator clearly led to an increase in the rate of consumption of portlandite for both UFA5 and MUFA5 hybrids, but more so for the MUFA5 hybrid for which activation methods were combined. This agrees with the XRD findings on portlandite consumption and the degree of pozzolanic activity of the coal fly ash specimens.

3.3.3. Fourier Transform Infrared Spectroscopy

FTIR analysis of the hydration products at different hydration ages obtained for the four hybrid cement pastes (UFA, UFA5, MUFA and MUFA5) is shown in Figures 8 and 9. The spectra for the unreacted starting materials (UFA, MUFA and MC) are included for comparison with the hybrid cements after hydration.

In comparison to the transmission spectrum of raw cement (MC) at the bottom of Figure 8b, a new transmission band has evolved in the spectrum of both the UFA and UFA5 hybrid cement specimens at around 960 cm^{-1}. The latter is already evident after only 1 day of hydration and occurs through all hydration ages tested. This band (960 cm^{-1}) has been described in literature to represent the Si-O asymmetric stretching vibration (v_3) of the calcium silicate hydration product, also referred to as C-S-H gel, produced during cement hydration. This is the only gel phase clearly distinguishable in the FTIR data of the four hybrid cements. The position of this band does not appear to move to higher wavenumbers as suggested in literature, indicating the progress of hydration and polymerisation of Si-O [48]. It does however appear to increase in relative intensity with increasing curing age, suggesting an increase in the quantity of this specific hydration product. The exact position of the main Si-O band depends on the Ca/Si ratio of the C-S-H gel produced during hydration [6,37,48]. The presence of molecular water, represented by a weak absorption band between 1600 and 1700 cm^{-1} (O-H bend), is evident at all curing ages.

Another product of cement hydration, ettringite, is visible for both scenarios (UFA and UFA5) at 1113 cm^{-1}. This band is associated with SO_4^{2-} stretching vibrations (v_3) usually found between 1100 and 1170 cm^{-1} [48]. Once chemical activation is applied to the UFA hybrid (UFA5, Figure 8b), an increase in the relative intensity of the ettringite band (1113 cm^{-1}) is observed through all curing ages. This phenomenon of increased ettringite formation after chemical activation with Na_2SO_4 serves as an indication of the formation of stable, well crystallised ettringite needles, and supports the XRD and DTG findings and discussions. The same can be said for the hybrid cements where the coal fly ash has been mechanically activated (MUFA, Figure 9a) and a combination of chemical and mechanical activation was applied (MUFA5, Figure 9b). Once again, the addition of Na_2SO_4 improved the relative intensity of the ettringite band.

Apart from the new bands representing C-S-H gel, ettringite and molecular water (O-H bend) that appear after hydration, the remainder of the bands occurring in the FTIR spectra of the hydrated samples can be attributed to contributions from the starting materials e.g., carbonates [25].

The FTIR transmission band in the 2000–4000 cm^{-1} range of significant concern for this study is the small, sharp band at around 3641–3642 cm^{-1} ascribed to O-H stretching of $Ca(OH)_2$ (portlandite) [48,49]. Figure 10 compares the occurrence of this band for the four hybrid cement pastes after 1 day and 28 days of hydration.

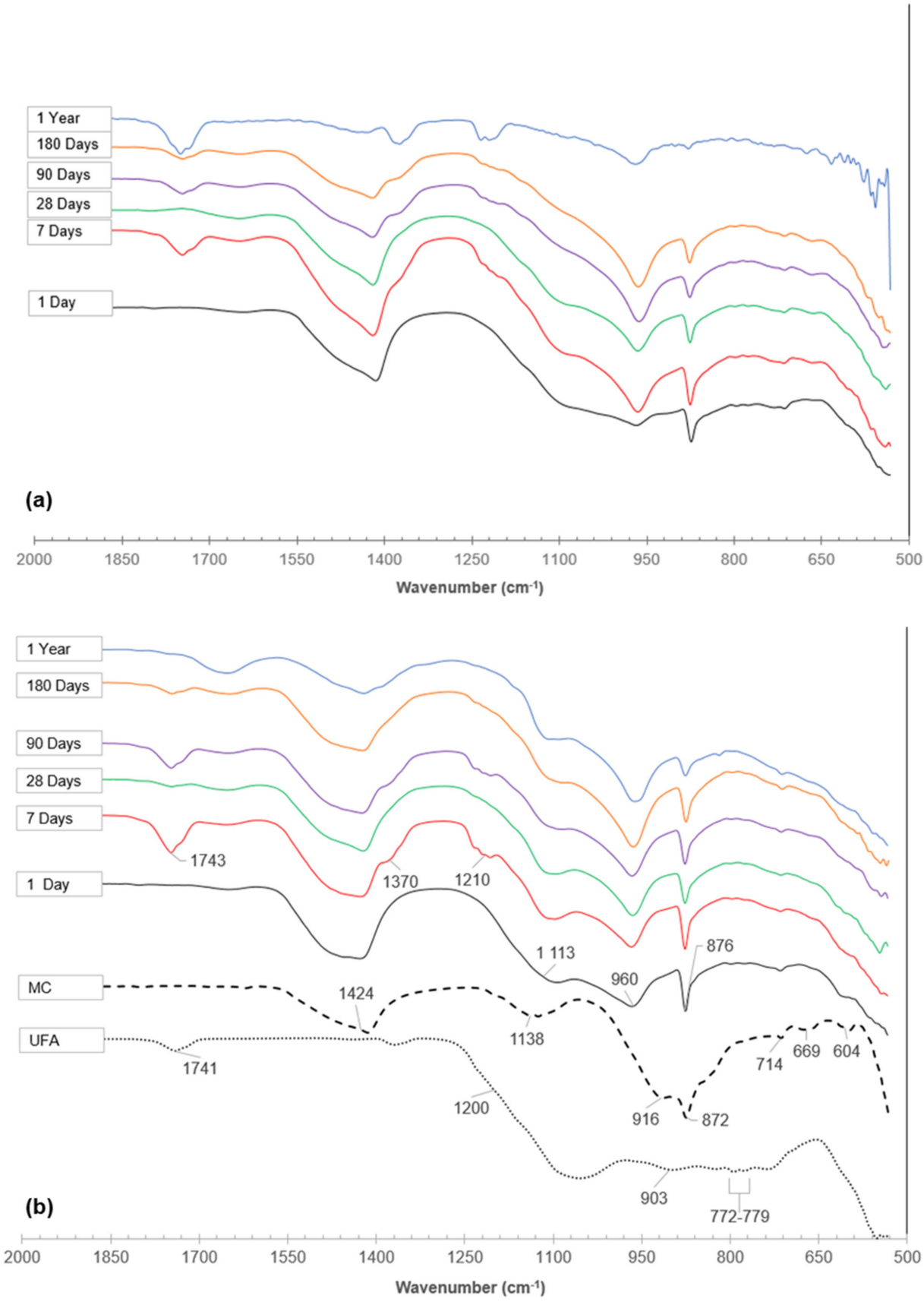

Figure 8. FTIR transmission spectra between wavenumbers 530–2000 cm^{-1} for the (**a**) UFA and (**b**) UFA5 hybrid cements at all hydration ages tested.

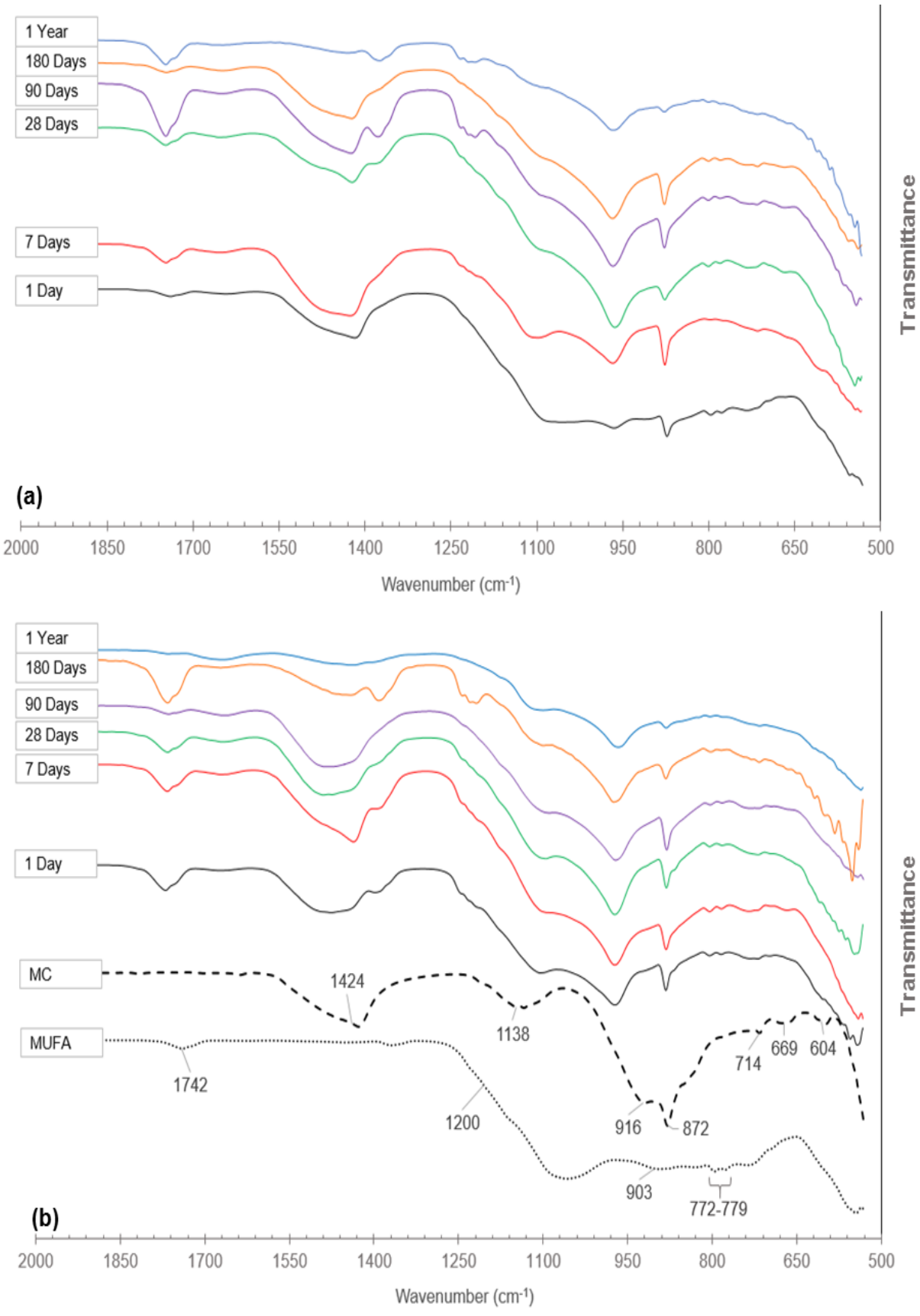

Figure 9. FTIR transmission spectra between wavenumbers 530–2000 cm^{-1} for the (**a**) MUFA and (**b**) MUFA5 hybrid cements at all hydration ages tested.

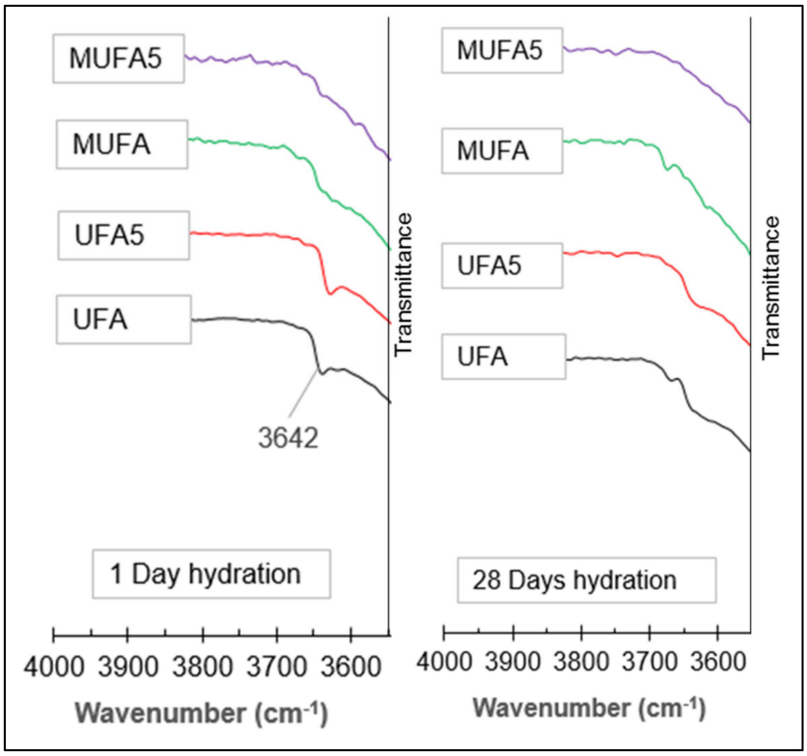

Figure 10. FTIR transmission spectra for the hydrated cement pastes (UFA, UFA5, MUFA and MUFA5) between 3600–4000 cm^{-1} after 1 day and 28 days of hydration.

It is evident that after 1 day of hydration, mechanical activation (MUFA), and especially the combination of chemical and mechanical activation (MUFA5) increases the rate of pozzolanic activity of the coal fly ash, evident by the disappearance of the portlandite band at 3642 cm^{-1}. Once the samples have hydrated for 28 days, there is no more evidence of the small sharp band associated to portlandite. The latter may be due to the portlandite being either completely consumed, or its quantity being so small that it is not clearly evident on the spectra anymore. This trend of increased pozzolanic activity of fly ash was however also found and supported by the XRD and DTG results.

3.4. The Effect of Chemical and Mechanical Activation on the Pozzolanic Reactivity of Coal Fly Ash in a High Coal Fly Ash Hybrid Cement

Pozzolanic reactivity of coal fly ash in this discussion will refer to the rate at which portlandite is consumed within the different coal fly ash hybrid cements. Figure 11 summarises the XRD and DTG data presenting the occurrence of portlandite, to serve as indication of the degree of the pozzolanic reaction (reactivity) of hydrated coal fly ash hybrid cement specimens upon chemical and mechanical activation.

With no activation applied to the hybrid cement paste (UFA), portlandite is still evident at 28 days, and a small XRD peak ($2\Theta = 21.0°$) was even identified at 90 days as previously shown in Figure 4a. Once chemical activation is applied to the hybrid cement paste (UFA5), portlandite was mostly consumed at 28 days. Applying mechanical activation to the unclassified coal fly ash (MUFA) resulted in an even faster pozzolanic reaction compared to the application of only chemical activation (Na_2SO_4) to the unclassified coal fly ash. The relative peak intensities significantly reduced, and no portlandite was evident at 28 days. By combining the activation methods to the hybrid cement paste (MUFA5), the fastest pozzolanic reaction was achieved, with portlandite evident at 1 day, but consumed at the fastest rate compared to the other hybrids.

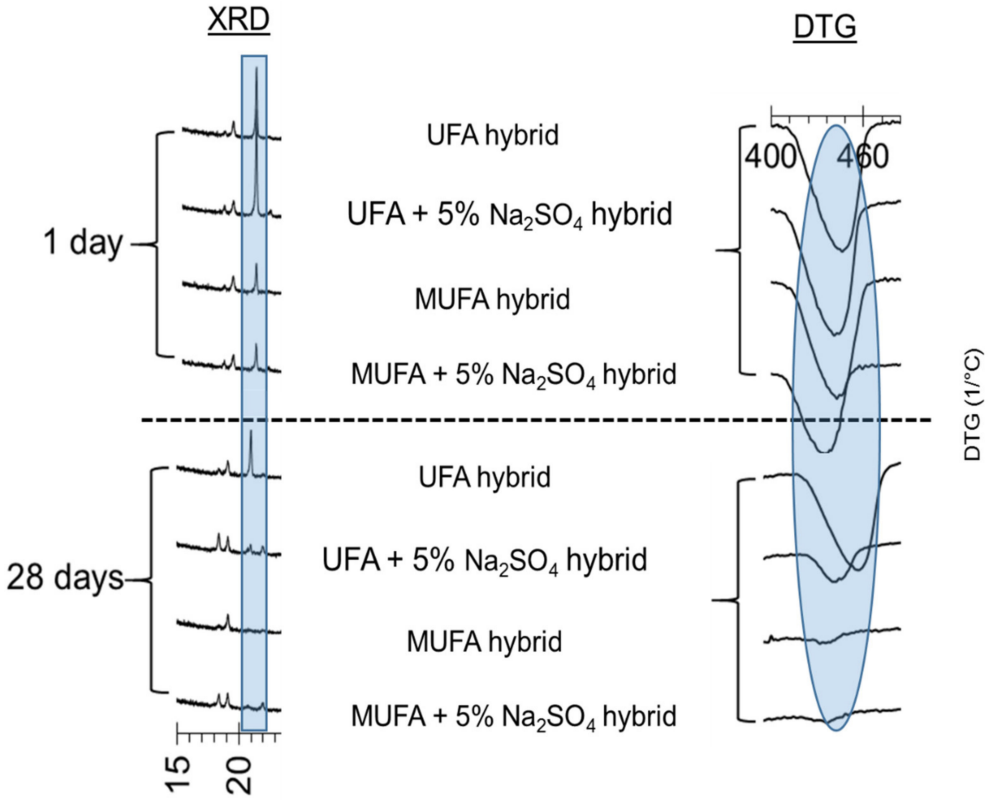

Figure 11. Summary of XRD and DTG data presenting the consumption of portlandite as an indication of the pozzolanic reaction of hydrated coal fly ash hybrid cement upon chemical and mechanical activation.

These results serve as evidence that activation of coal fly ash, more specifically the combination of chemical and mechanical activation, enhances the reactivity of the hybrid system by improving the rate of initiation of the pozzolanic reaction between coal fly ash and portlandite. DTG and XRD results clearly showed the consumption of portlandite after specific curing ages. The order of pozzolanic reactivity of coal fly ash for the four hybrid cement scenarios tested in this study are subsequently summarised as follows:

$$\text{UFA} < \text{UFA} + 5\%\ Na_2SO_4 < \text{MUFA} < \text{MUFA} + 5\%\ Na_2SO_4$$

3.5. The effect of Chemical and Mechanical Activation on Stable Ettringite Formation in a High Coal Fly Ash Hybrid Cement

It has been reported that the formation of well crystallized, stable ettringite will lend to an increase in paste volume, leading to a denser matrix and hence an increase in compressive strength [17,18]. The size of the ettringite crystals is also a very important aspect to keep in mind with regard to its stability, i.e., small, poorly crystallized crystals will tend to dissolve more easily compared to large, well-formed crystals [50]. The analytical techniques used in this study which was able to identify ettringite, all agreed on the existence of ettringite for all four hybrid cement scenarios, at all of the studied curing ages, even up to 1 year. Figure 12 provides a summary of the XRD and DTG data, indicating the presence of ettringite in hydrated coal fly ash hybrid cement specimens upon chemical and mechanical activation.

The relative XRD and DTA (Figure 12) peak intensities clearly showed that the addition of Na_2SO_4 to the hybrid cement paste (UFA5) promotes ettringite formation when compared to no activation (UFA) [40]. Interestingly enough, when the application of mechanical activation without chemical activation (MUFA) is applied and compared, it does not appear to contribute to increased ettringite formation.

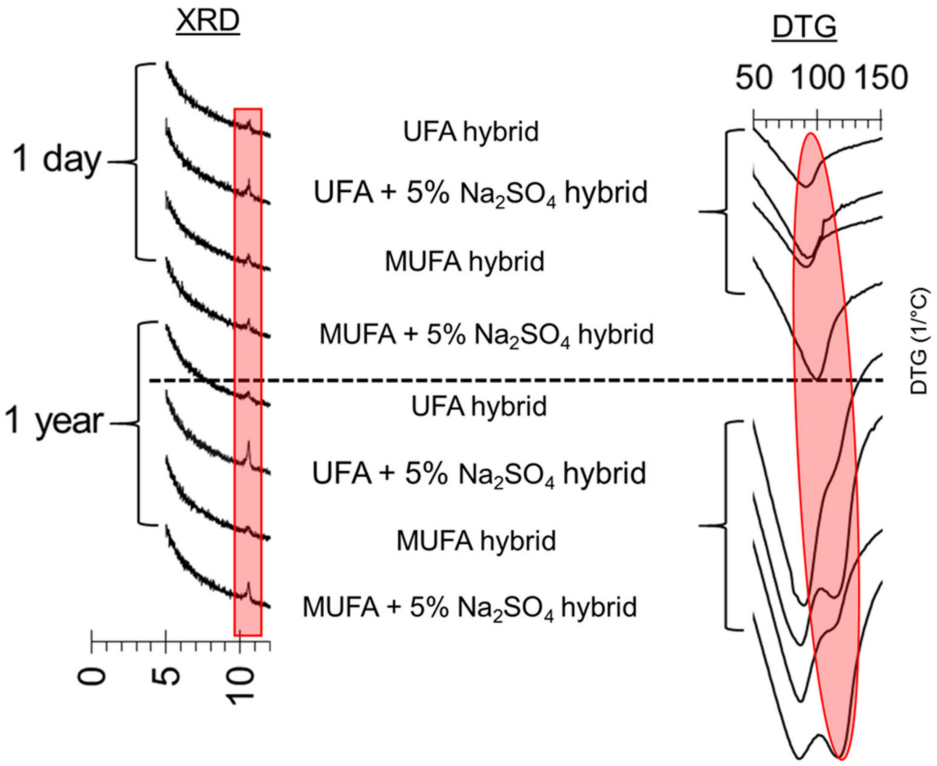

Figure 12. Summary of XRD and DTG data presenting the presence of ettringite in hydrated coal fly ash hybrid cement specimens upon chemical and mechanical activation.

From the results presented, it would appear that in comparison to mechanical activation, chemical activation (Na_2SO_4) plays a critical role in the formation of well crystallized, stable ettringite within the hydrated hybrid cement. For the purpose of this study, stable ettringite refers to it not converting to monosulfoaluminate, or "disappearing" after a few hours or days as suggested by some literature [6,33]. This is also evident once activation methods are combined (MUFA5). The relative peak intensities for the combined activation methods present similar intensities in comparison to the hybrid which only had chemical activation applied (UFA5), implying no significant additional contribution evident from mechanical activation towards ettringite formation.

Since it was just deliberated that mechanical activation makes little to no contribution to ettringite formation, any favourable physical performance from the combination of activation methods must then be a result of promoted ettringite formation from chemical activation, in combination with other factors and advantages from mechanical activation like an increase in the rate of pozzolanic activity between coal fly ash and cement.

The existence of monocarboaluminate was evident for both UFA and MUFA hybrids where Na_2SO_4 was not used as a chemical activator. Once Na_2SO_4 was added to both of these systems, the monocarboaluminate was no longer evident. This would suggest that in specimens with no added Na_2SO_4, the sulfate content was still sufficient to prevent conversion of the ettringite to monosulfoaluminate, and rather produce monocarboaluminate from 7 days onwards. These findings are in agreement with the hydration chemistry of coal fly ash containing cements [25]. Since ettringite formation is favoured by the presence of sulfates, no AFm phases were evident once Na_2SO_4 was added [16]. No monosulfoaluminate was detected in any of the four hybrid cases, confirming there was no conversion of ettringite to monosulfoaluminate [18].

It would appear that the reaction conditions in this study, whether chemical or mechanical activation was applied to the system, promoted the production of well crystallized, stable ettringite, which agrees with Velandia et al. [22] who also found ettringite formation to be favoured by Na_2SO_4 addition.

It is also well known that small ettringite crystals can undergo a process called "Ostwald ripening". This is the scenario where small ettringite crystals precipitate in large pores where favourable conditions result in the growth of larger, more stable crystals [6,16]. An example of this process is shown in Figure 13 with the addition of Na_2SO_4 where well crystallized ettringite crystals formed in voids within the hydrated hybrid cement matrix, improving the density of the hydrated cement compared to samples containing no additional sulphates. It was previously reported that the addition of sulphate activators into fly ash-cement pastes, changes the pore distribution, resulting in smaller pore size and lower porosity [40]. All four micrographs are of the UFA5 hybrid at a very late hydration age (180 days), proving stable ettringite formation within this specific hybrid even at later curing ages.

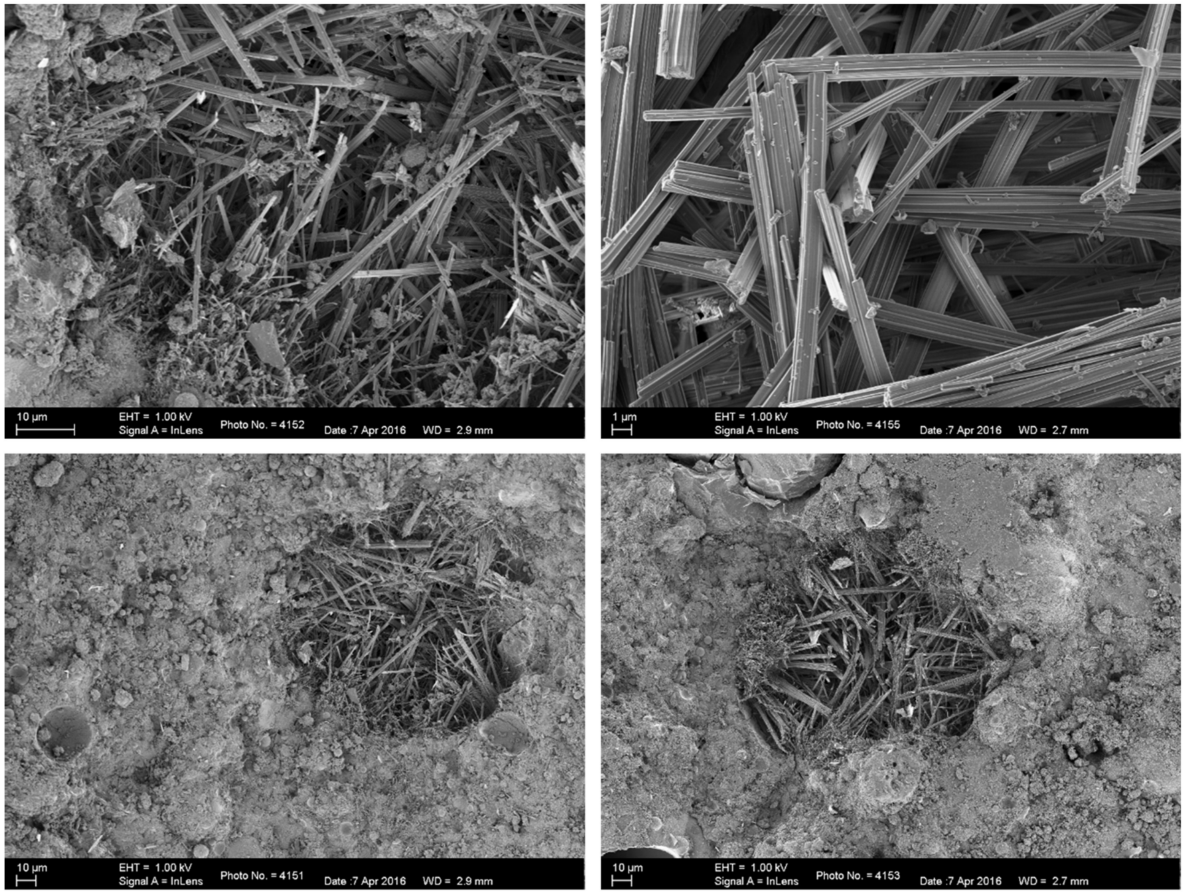

Figure 13. Well crystallized ettringite needles in the UFA5 hybrid at 180 days of curing.

4. Conclusions

These results proved that chemical activation of hybrid cements by means of Na_2SO_4 addition, increases the degree of stable, well crystallised ettringite formation, which may lead to denser hybrid specimens with increased strength. It was found that, compared to chemical activation on its own, the combination of activation techniques did not result in increased ettringite formation. The distinct presence of monocarboaluminate where no chemical activation was applied, was no longer evident when Na_2SO_4 was used to chemically activate the coal fly ash hybrid cement. There was no evidence of ettringite converting to monosulfoaluminate in any of the scenarios. Larger, more stable ettringite crystals also precipitated in large pores where conditions were favourable.

Chemical activation as well as mechanical activation increased the rate at which portlandite was consumed, which is furthermore indicative of an increase in the rate of the pozzolanic reaction between portlandite contained in cement and coal fly ash. However,

the application of combined chemical and mechanical activation definitely resulted in the fastest rate of portlandite consumption, hence an increased rate of the pozzolanic reaction. The order of pozzolanic reactivity of coal fly ash for the four hybrid cement scenarios were as follows: UFA < UFA + 5% Na_2SO_4 < MUFA < MUFA + 5% Na_2SO_4.

All four of the hybrid cement pastes proved to contain C-S-H-type gel in accordance with normal cement hydration. The results did not suggest any possible polymerisation of Si-O for the C-S-H gel, but rather showed an increase in quantity with increasing curing. Evidence of additional types of gel that may have formed, was not evident.

Author Contributions: G.d.T., conceptualization, data curation, formal analysis, investigation, methodology, project administration, validation, visualization, writing—original draft. E.M.v.d.M., resources, supervision, validation, writing—review & editing. R.A.K., validation, writing—review & editing. J.M.M., funding acquisition, resources, supervision. E.P.K., resources, supervision, validation, writing—review & editing. All authors have read and agreed to the published version of the manuscript.

Funding: The project was financially supported by the National Research Foundation of South Africa (NRF; grant No. TP14072580026). Any opinion, finding and conclusion or recommendation expressed in this material is from the authors, and the NRF does not accept any liability in this regard.

Acknowledgments: The author acknowledges the financial aid and study opportunity from AfriSam (South Africa) (Pty) Ltd., and also for making their laboratory resources and equipment available. Ms Wiebke Grote (University of Pretoria) is acknowledged for the XRD analyses, and the University of Pretoria Laboratory for Microscopy and Microanalysis for assistance with FESEM. Barbara Lothenbach (Empa—Swiss Federal for Materials Science and Technology) is acknowledged for her assistance with the interpretation of XRD and TGA/DTG results.

Conflicts of Interest: The authors declare that they have no known competing financial interest or personal relationships that could have appeared to influence the work reported in this paper.

List of Abbreviations and Notations

FA	coal fly ash
UFA	unclassified coal fly ash (d_{50}: approximately 60 μm)
UFA5	chemically activated unclassified coal fly ash
MUFA	mechanically activated unclassified coal fly ash (d_{50}: approximately 7 μm)
MUFA5	chemically and mechanically activated unclassified coal fly ash
MC	anhydrous Portland cement
CH	calcium hydroxide ($Ca(OH)_2$)
CS	calcium sulphate ($CaSO_4$)
(N,C)–A–S–H gel	sodium–calcium–aluminate–silicate hydrate
C3A	calcium aluminate phase
AFm	monosulfoaluminate

References

1. Miller, S.A.; John, V.M.; Pacca, S.A.; Horvath, A. Carbon dioxide reduction potential in the global cement industry by 2050. *Cem. Concr. Res.* **2018**, *114*, 115–124. [CrossRef]
2. Shi, C.; Jiménez, A.F.; Palomo, A. New cements for the 21st century: The pursuit of an alternative to Portland cement. *Cem. Concr. Res.* **2011**, *41*, 750–763. [CrossRef]
3. Donatello, S.; Garcia-Lodeiro, I.; Fernandez-Jimenez, A.; Palomo, A. Some durability aspects of hybrid alkaline cements. In *MATEC Web of Conferences*; EDP Sciences: Les Ulis, France, 2014; Volume 11, p. 01008. [CrossRef]
4. Garcia-Lodeiro, I.; Fernández-Jimenez, A.; Palomo, A. Cements with a low clinker content: Versatile use of raw materials. *J. Sustain. Cem.-Based Mater.* **2015**, *4*, 140–151. [CrossRef]
5. Donatello, S.; Fernández-Jimenez, A.; Palomo, A.; Jantzen, C. Very High Volume Fly Ash Cements. Early Age Hydration Study Using Na_2SO_4 as an Activator. *J. Am. Ceram. Soc.* **2013**, *96*, 900–906. [CrossRef]
6. Donatello, S.; Maltseva, O.; Fernandez-Jimenez, A.; Palomo, A.; Klein, L. The Early Age Hydration Reactions of a Hybrid Cement Containing a Very High Content of Coal Bottom Ash. *J. Am. Ceram. Soc.* **2014**, *97*, 929–937. [CrossRef]
7. Kovtun, M.; Kearsley, E.P.; Shekhovtsova, J. Dry powder alkali-activated slag cements. *Adv. Cem. Res.* **2015**, *27*, 447–456. [CrossRef]

8. Shekhovtsova, J.; Kovtun, M.; Kearsley, E.P. Temperature rise and initial shrinkage of alkali-activated fly ash cement pastes. *Adv. Cem. Res.* **2016**, *28*, 3–12. [CrossRef]
9. Blanco, F.; Garcia, M.P.; Ayala, J.; Mayoral, G.; Garcia, M.A. The effect of mechanically and chemically activated fly ashes on mortar properties. *Fuel* **2006**, *85*, 2018–2026. [CrossRef]
10. Heinz, D.; Göbel, M.; Hilbig, H.; Urbonas, L.; Bujauskaite, G. Effect of TEA on fly ash solubility and early age strength of mortar. *Cem. Concr. Res.* **2010**, *40*, 392–397. [CrossRef]
11. Wilińska, I.; Pacewska, B.; Ostrowski, A. Investigation of different ways of activation of fly ash–cement mixtures. *J. Therm. Anal. Calorim.* **2019**, *138*, 4203–4213. [CrossRef]
12. Scrivener, K.; Martirena, F.; Bishnoi, S.; Maity, S. Calcined clay limestone cements (LC 3). *Cem. Concr. Res.* **2017**, *114*, 49–56. [CrossRef]
13. Palomo, A.; Krivenko, P.; Garcia-Lodeiro, I.; Kavalerova, E.; Maltseva, O.; Fernández-Jiménez, A. A review on alkaline activation: New analytical perspectives. *Mater. Constr.* **2014**, *64*, e022. [CrossRef]
14. Garcia-Lodeiro, I.; Donatello, S.; Fernández-Jiménez, A.; Palomo, Á. Hydration of Hybrid Alkaline Cement Containing a Very Large Proportion of Fly Ash: A Descriptive Model. *Materials* **2016**, *9*, 605. [CrossRef]
15. Qiao, X.C.; Poon, C.S.; Cheung, E. Comparative studies of three methods for activating rejected fly ash. *Adv. Cem. Res.* **2006**, *18*, 165–170. [CrossRef]
16. Garcia-Lodeiro, I.; Taboada, V.C.; Fernández-Jiménez, A.; Palomo, Á. Recycling Industrial By-Products in Hybrid Cements: Mechanical and Microstructure Characterization. *Waste Biomass Valorization* **2016**, *8*, 1433–1440. [CrossRef]
17. Qian, J.; Shi, C.; Wang, Z. Activation of blended cements containing fly ash. *Cem. Concr. Res.* **2001**, *31*, 1121–1127. [CrossRef]
18. Fernández-Jiménez, A.; Sobrados, I.; Sanz, J.; Palomo, A. Hybrid cements with very low OPC content. In Proceedings of the International Congress on the Chemistry of Cement ICCC XIII, Madrid, Spain, 3–8 July 2011.
19. Kumar, S.; Kumar, R. Mechanical activation of fly ash: Effect on reaction, structure and properties of resulting geopolymer. *Ceram. Int.* **2011**, *37*, 533–541. [CrossRef]
20. Kumar, R.; Kumar, S.; Mehrotra, S.P. Towards sustainable solutions for fly ash through mechanical activation. *Resour. Conserv. Recycl.* **2007**, *52*, 157–179. [CrossRef]
21. Pacewska, B.; Wilińska, I. Comparative investigations of influence of chemical admixtures on pozzolanic and hydraulic activities of fly ash with the use of thermal analysis and infrared spectroscopy. *J. Therm. Anal. Calorim.* **2014**, *120*, 119–127. [CrossRef]
22. Velandia, D.F.; Lynsdale, C.J.; Provis, J.L.; Ramirez, F.; Gomez, A.C. Evaluation of activated high volume fly ash systems using Na_2SO_4, lime and quicklime in mortars with high loss on ignition fly ashes. *Constr. Build. Mater.* **2016**, *128*, 248–255. [CrossRef]
23. Joseph, S.; Snellings, R.; Cizer, Ö. Activation of Portland cement blended with high volume of fly ash using Na_2SO_4. *Cem. Concr. Compos.* **2019**, *104*, 103417. [CrossRef]
24. Du Toit, G.; Kearsley, E.P.; Mc Donald, J.M.; Kruger, R.A.; van der Merwe, E.M. Chemical and mechanical activation of hybrid fly ash cement. *Adv. Cem. Res.* **2018**, *30*, 399–412. [CrossRef]
25. Du Toit, G. Chemical and Mechanical Activation of Hybrid Fly Ash Cement. Ph.D. Thesis, University of Pretoria, Pretoria, South Africa, 2018.
26. Deschner, F.; Winnefeld, F.; Lothenbach, B.; Seufert, S.; Schwesig, P.; Dittrich, S.; Goetz-Neunhoeffer, F.; Neubauer, J. Hydration of Portland cement with high replacement by siliceous fly ash. *Cem. Concr. Res.* **2012**, *42*, 1389–1400. [CrossRef]
27. Scholer, A.; Lothenbach, B.; Winnefeld, F.; Zajac, M. Hydrate formation in quaternary Portland cement blends containing blast-furnace slag, siliceous fly ash and limestone powder. *Cem. Concr. Compos.* **2015**, *55*, 374–382. [CrossRef]
28. Scrivener, K.; Snellings, R.; Lothenbach, B. *A Practical Guide to Microstructural Analysis of Cementitious Materials*, 1st ed.; Scrivener, K., Snellings, R., Lothenbach, B., Eds.; CRC Press: Boca Raton, FL, USA, 2016.
29. *EN 196-1:2016*; Methods of Testing Cemen—Part 1: Determination of Strength. CEN: Brussels, Belgium, 2016.
30. Paul, K.T.; Satpathy, S.K.; Manna, I.; Chakraborty, K.K.; Nando, G.B. Preparation and Characterization of nano structured materials from fly ash: A waste from thermal power stations, by high energy ball milling. *Nanoscale Res. Lett.* **2007**, *2*, 397–404. [CrossRef]
31. Patil, A.G.; Anandhan, S. Ball milling of class-f indian fly ash obtained from a thermal power station. *Int. J. Energy Eng.* **2012**, *2*, 57–62.
32. Kearsley, E.P.; Wainwright, P.J. Effect of fly ash properties on concrete strength. *J. South Afr. Inst. Civ. Eng.* **2003**, *45*, 19–24.
33. Hewlett, P. *Lea's Chemistry of Cement and Concrete*, 4th ed.; Elsevier Science & Technology Books: Amsterdam, The Netherlands, 2004.
34. *EN 197-1; CEN*; Cement—Part 1: Composition, Specifications and Conformity Criteria for Common Cements. CEN: Brussels, Belgium, 2011.
35. Fernández-Jiménez, A.; Palomo, A. Characterisation of fly ashes. Potential reactivity as alkaline cements. *Fuel* **2003**, *82*, 2259–2265. [CrossRef]
36. Criado, M.; Jiménez, A.F.; Palomo, A. Effect of sodium sulfate on the alkali activation of fly ash. *Cem. Concr. Compos.* **2010**, *32*, 589–594. [CrossRef]
37. Palomo, A.; Fernández-Jiménez, A.; Kovalchuk, G.; Ordoñez, L.M.; Naranjo, M.C. Opc-fly ash cementitious systems: Study of gel binders produced during alkaline hydration. *J. Mater. Sci.* **2007**, *42*, 2958–2966. [CrossRef]
38. García-Lodeiro, I.; Fernández-Jiménez, A.; Palomo, A. Hydration kinetics in hybrid binders: Early reaction stages. *Cem. Concr. Compos.* **2013**, *39*, 82–92. [CrossRef]

39. García-Lodeiro, I.; Fernández-Jiménez, A.; Palomo, A. Variation in hybrid cements over time. Alkaline activation of fly ash–portland cement blends. *Cem. Concr. Res.* **2013**, *52*, 112–122. [CrossRef]
40. Lee, C.Y.; Lee, H.K.; Leeb, K.M. Strength and microstructural characteristics of chemically activated fly ash–cement systems. *Cem. Concr. Res.* **2003**, *33*, 425–431. [CrossRef]
41. Shi, C.; Day, R.L. Acceleration of the reactivity of fly ash by chemical activation. *Cem. Concr. Res.* **1995**, *25*, 15–21. [CrossRef]
42. Pacewska, B.; Wilińska, I. Usage of supplementary cementitious materials: Advantages and limitations. *J. Therm. Anal. Calorim.* **2020**, *142*, 371–393. [CrossRef]
43. Wilińska, I.; Pacewska, B. Influence of selected activating methods on hydration processes of mixtures containing high and very high amount of fly ash. *J. Therm. Anal. Calorim.* **2018**, *133*, 823–843. [CrossRef]
44. Ubbrìaco, P.; Bruno, P.; Traini, A.; Calabrese, D. Fly ash reactivity. Formation of hydrate phases. *J. Therm. Anal. Calorim.* **2001**, *66*, 293–305. [CrossRef]
45. Alahrache, S.; Winnefeld, F.; Champenois, J.-B.; Hesselbarth, F.; Lothenbach, B. Chemical activation of hybrid binders based on siliceous fly ash and Portland cement. *Cem. Concr. Compos.* **2016**, *66*, 10–23. [CrossRef]
46. Herath, C.; Gunasekara, C.; Law, D.W.; Setunge, S. Long term mechanical performance of nano-engineered high volume fly ash concrete. *J. Build. Eng.* **2021**, *43*, 103168. [CrossRef]
47. Duvallet, T.; Rathbone, R.F.; Henke, K.R.; Jewell, R.B. Low-Energy, Low CO_2-Emitting Cements Produced from Coal Combustion By-Products and Red Mud. In Proceedings of the 2009 World of Coal Ash (WOCA) Conference, Lexington, KY, USA, 22–25 April 2009.
48. Kontoleontos, F.; Katsiotisa, N.; Tsakiridisb, P.; Kaloidasc, V.; Marinosa, A.; Katsiotia, M. Dry-grinded Ultrafine Cements Hydration. Physicochemical and Microstructural Characterization. *Mater. Res.* **2013**, *16*, 404–416. [CrossRef]
49. Mollah, M.Y.A.; Yu, W.; Schennach, R.; Cocke, D.L. A Fourier transform infrared spectroscopic investigation of the early hydration of Portland cement and the influence of sodium lignosulfonate. *Cem. Concr. Res.* **2000**, *30*, 267–273. [CrossRef]
50. Chrysochoou, M.; Dermatas, D. Evaluation of ettringite and hydrocalumite formation for heavy metal immobilization: Literature review and experimental study. *J. Hazard Mater.* **2006**, *136*, 20–33. [CrossRef] [PubMed]